Improved magnetoelectric performance of the Ni-P/Ni/Pb(Zr,TiO)$_3$ cylindrical layered composites

D. A. Pan,[1,a)] J. Wang,[1] Z. J. Zuo,[1] S. G. Zhang,[1] B. Liu,[1] A. A. Volinsky,[2] and L. J. Qiao[1]
[1]*Institute of Advanced Materials and Technology, University of Science and Technology Beijing, Beijing 100083, China*
[2]*Department of Mechanical Engineering, University of South Florida, Tampa, Florida 33620, USA*

(Received 28 July 2014; accepted 24 August 2014; published online 8 September 2014)

The Ni-P/Ni/Pb(Zr,TiO)$_3$ (PZT) cylindrical layered magnetoelectric (ME) composites have been prepared by electroless deposition and electrodeposition. The ME effect in the axial mode was researched in this paper. Compared with that of the Ni/PZT and Ni-P/PZT composites, the Ni-P/Ni/PZT composites have both lower optimal magnetic field and higher ME voltage coefficient. The reason for the ME improvement can be ascribed to the flux concentration effect and the compressive stress in the Ni layers induced by the high permeability Ni-P layers. These results open up a suitable way to enhance the sensitivity and optimize the design of ME devices for practical application. © *2014 AIP Publishing LLC*. [http://dx.doi.org/10.1063/1.4895065]

The magnetoelectric (ME) effect is defined as an induced dielectric polarization under an applied magnetic field (H) and/or an induced magnetization under an external electric field (E).[1] The laminated ME materials have attracted renewed interest for both their fundamental physical properties and potential applications as sensors, actuators, transducers, etc.[2–8] Currently, there are multiple methods available for preparing laminated ME composites with different kinds of interfacial bonding, including bonding with epoxy, electrodeposition, and electroless deposition.[9–12]

Improving magnetoelectric device characteristics can be achieved by enhancing the ME response of laminated composite, DC magnetic field sensitivity of the ME voltage coefficient, and reducing the optimal bias magnetic field. Zuo *et al.*[13] reported Terfenol-D/Pb(Zr,TiO)$_3$ (PZT)/Terfenol-D laminated ME composites with very high ME voltage coefficient of ~10 V/cm·Oe by bonding PZT and Terfenol-D disks with epoxy. However, high DC magnetic bias, H_{DC}, was required to obtain the maximum ME voltage coefficient. Trying to achieve giant ME properties in laminates under low bias magnetic field, Dong *et al.*[14] found that the required DC magnetic bias can be significantly altered by the incorporation of μ-metal layers into laminate composites of Terfenol-D and PZT. Using the flux concentration effect of Metglas, Zhai *et al.*[15] reported the ME coefficient of 7.2 V/cm·Oe at 8 Oe static magnetic field with 1 kH frequency in the Metglas layers laminated together with polyvinylidenefluoride (PVDF) piezopolymer layers. Afterwards, Fang *et al.*[16] obtained the ME coefficient of up to 21.5 V/cm·Oe for the Metglas/PVDF bilayered laminates under alternating magnetic field at 20 Hz. These results demonstrate a significant enhancement in the ME voltage coefficient at low bias magnetic field. Based on the inference, the method of flux concentration offers a unique approach to enhancing the sensitivity and directionality of the ME magnetic sensors.[16]

Under an applied magnetic field, $\boldsymbol{H}$, the magnetic induction, $\boldsymbol{B} = (\mu_0\mu_r\boldsymbol{H})$, inside a ferromagnetic material is strongly related to that material's relative permeability, $\boldsymbol{\mu_r}$.[14] Thus, high permeability acting on the laminated ME structure can reduce the optimal bias magnetic field of this structure via magnetic flux concentration. Nickel is a kind of universal strong magnetic material, while Ni-P alloy has amorphous nanocrystalline structure exhibiting new properties as high magnetic induction, high permeability and low loss.[17,18] Besides, it is convenient to prepare Ni and Ni-P alloys by electrodeposition and electroless deposition, respectively. These methods can avoid the disadvantages of nonrigid contact, fatigue and aging effect due to the polymer binder.[19] In order to attain both high magnetoelectric effect and low optimal bias magnetic field, Ni-P/Ni/PZT cylindrical layered ME composites have been prepared, achieving stronger ME coupling in the ME composite at lower $H_{dc,opt}$ by incorporating high-permeability ferromagnetic Ni-P layers.

The PZT cylinders with the $\Phi 20 \times \Phi 18 \times 10\,mm^3$ dimensions were polarized along the radial direction after electroplating a thin Ni layer on its inside and outside surfaces. The pretreatment process applied prior to the electroplated Ni and the electroless Ni-P consisted of supersonic cleaning and sulfuric acid cathodic activation. The bath composition and the deposition conditions of Ni electrodeposition and Ni-P electroless deposition are presented in detail elsewhere.[11,17] The phosphorus content of the Ni-P layers is approximately 7.78 wt. % with no impurities present, and the Ni-P layers have both micro-crystalline and amorphous structure.[17] For comparison, the Ni/PZT, Ni-P/PZT, and Ni-P/Ni/PZT cylindrical layered composites were prepared and their geometrical arrangements are shown Schematically in Fig. 1. Each sample has approximately the same magnetostrictive thickness and the specific dimensions are listed in Table I.

The ME effect of the prepared composites was measured in the ME measurement system, where both constant (H_{DC}) and alternating (δH) magnetic fields were applied parallel (axial mode) to the cylinder height direction. The ME voltage coefficient was calculated as $\alpha_E = \delta V/(t_{PZT}\cdot\delta H)$, where

[a)]Author to whom correspondence should be addressed. Electronic mail: pandean@mater.ustb.edu.cn. Tel.: +8610-82376835. Fax: +8610-62333375.

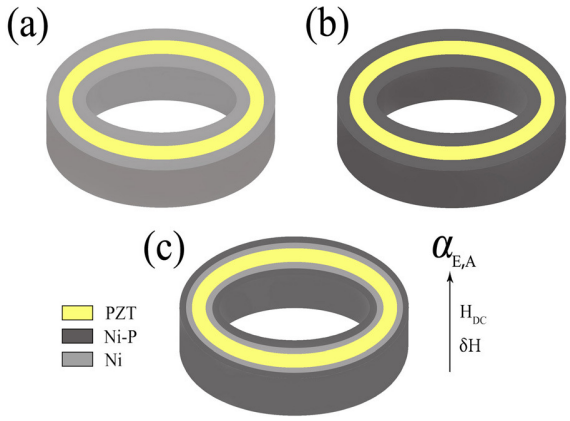

FIG. 1. Schematic illustration of the geometrical arrangement of: (a) Ni/PZT; (b) Ni-P/PZT, and (c) Ni-P/Ni/PZT/ cylinders.

t_{PZT} is the PZT layer thickness and δH is the amplitude of the AC magnetic field generated by the Helmholtz coils. The AC current flowing through the coils with the applied magnetic field amplitude of $\delta H = 1.2$ Oe was equal to 1 A.[17]

The magnetic field frequency dependence of the ME voltage coefficient, $a_{E,A}$, at H_m (respective) for the Ni/PZT, Ni-P/PZT, and Ni-P/Ni/PZT composites is presented in Fig. 2(a). As shown in Fig. 2(a), all three composites have one resonance peak of $a_{E,A}$, appearing at 62.3 kHz, 60.6 kHz, and 62.7 kHz, respectively. The remarkable resonance peak is related to the electromechanical resonance.[20] The maximum $a_{E,A}$ value is 9 V/cm·Oe for the Ni-P/Ni/PZT composite. Fig. 2(b) shows the $\alpha_{E,A}$ dependence on the bias magnetic field, H_{DC}, at the respective resonance frequency. The $\alpha_{E,A}$ increased with H_{DC} until the local maximum value appeared at $H_{DC} = 500$, 140, and 380 Oe, in turn. Then, the $\alpha_{E,A}$ increased linearly with H_{DC} from the initial value of the linear region to 5 kOe. By comparison, for the Ni-P/Ni/PZT composite, it can be seen that the optimal magnetic field, $H_{dc,opt}$, is lower than that of the Ni/PZT composite, and the corresponding maximum value is larger than that of the other two composites.

TABLE I. Individual layer thicknesses of the samples.

Sample	Ni thickness	Ni-P thickness
Ni/PZT	720 μm	0 μm
Ni-P/PZT	0 μm	720 μm
Ni-P/Ni/PZT	400 μm	320 μm

In the axial coupling mode, the infinitesimal units suffer the magnetic field acting on the length direction under the applied magnetic field. The Ni-P/Ni/PZT cylindrical layered composite can be simplified as a differential plate laminated ME composite with the $h \times L^{eff} \times t$ dimensions, where t is the total thickness of the PE and PM phases, as shown in Fig. 3. With an applied magnetic field, H_{app} ($H_{dc} + H_{ac}$), the Ni layer and Ni-P layer are uniformly magnetized simultaneously. Due to the high permeability, the Ni-P layer can reach saturation magnetization under low magnetic field, and the magnetization, M, is almost independent of the applied magnetic field.[21] The Ni-P layer can be regarded as the source of static magnetic field, generating an additional magnetic field around it. Therefore, the effective magnetic intensity of the Ni layer is associated with the applied magnetic field and the additional generated magnetic field of the Ni-P layer, along with the demagnetizing factor.[21]

When the applied magnetic field exists, the internal effective magnetic field of the Ni layer increases on account of the high permeability of the Ni-P layer. It causes concentrated external flux in the Ni layer, resulting in stronger magnetic induction, $\boldsymbol{B} = \mu_0 \mu_r H$, in turn resulting in higher effective piezomagnetic coefficient under low magnetic field.[16] Thus, the $H_{dc,opt}$ of the Ni-P/Ni/PZT composites shifts to the left compared with the Ni/PZT composites, i.e., becomes lower. Moreover, both the inside and the outside Ni layers contract at the same time under the applied magnetic field in the Ni/PZT structure, so that the stress in the PZT ring is severely offset. However, In the Ni-P/Ni/PZT structure, the offsetting of the Ni-P layers is less that the Ni layers due to the small magnetostriction coefficient under the same

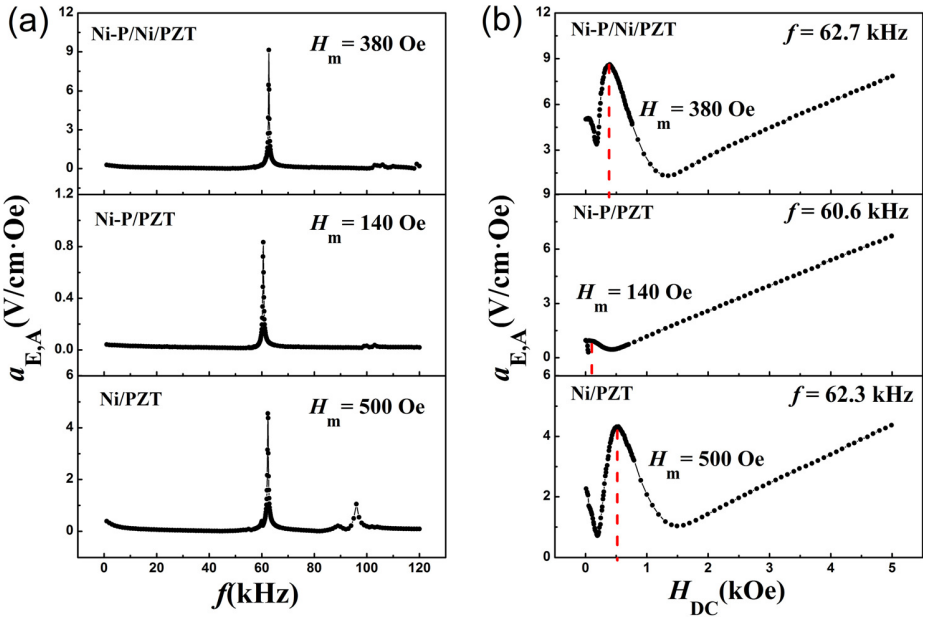

FIG. 2. (a) AC magnetic field frequency, f, dependence of $\alpha_{E,A}$ at the optimal magnetic field; (b) the H_{DC} dependence of $a_{E,A}$ at the resonance frequency.

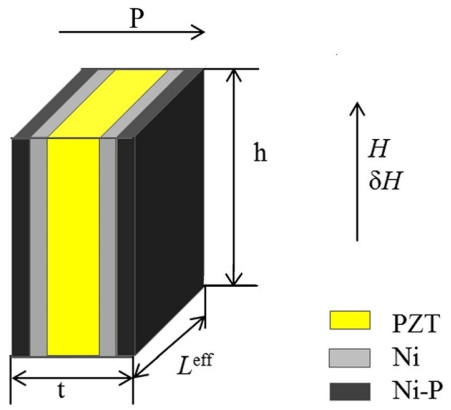

FIG. 3. Schematics of the corresponding model for the differential coefficient in the Ni-P/Ni/PZT cylindrical layered composite.

conditions and the same layer thickness. And, the Ni layers are surrounded by the Ni-P layers, making the free surface of Ni-P layers decrease and inducing better bondage effect. Therefore, the Ni-P layers produce compressive stress in the Ni layers under the applied magnetic field, causing Ni saturation magnetostriction coefficient to increase, further leading to the increase of the maximum ME voltage coefficient in the laminated structure (see Fig. 2(b)).

The higher ME voltage coefficient of Ni-P/Ni/PZT cylinder is a result of the complex configuration, stress, and boundary conditions of the Ni-P and Ni layers. The low $H_{dc,opt}$ may be attributed to the high permeability of the Ni-P alloy. Hence, the Ni-P/Ni/PZT composites have outstanding advantages of both high ME effect and low optimal magnetic field. These small sized Ni-P/Ni/PZT laminates can be widely used as miniature magnetic sensors, integrated microelectronic circuits, and various spurious noise and stray capacitor devices.[22]

In conclusion, the Ni-P/Ni/PZT cylindrical laminated structures have been made and studied. The ME voltage coefficient, $\alpha_{E,A}$, of this composite is up to 9 V/cm·Oe at the resonant frequency, which is higher than that of the Ni-P/PZT and the Ni/PZT composites. Its optimal magnetic field is at 380 Oe, lower than for the Ni/PZT composite. The higher $\alpha_{E,A}$ and the lower $H_{dc,opt}$ may be caused by the stress induced in the Ni layer and the high permeability of Ni-P layers, respectively. This composite has a great potential in the very high sensitivity magnetic sensor applications.

This work was supported by the Beijing Nova program (No. Z141103001814006), by the National Key Technology R&D Program (Nos. 2012BAC12B05 and 2012BAC02B01), by the National Natural Science Foundation of China (Nos. 51174247 and U1360202), by the National High-Tech Research and the Development Program of China (No. 2012AA063202).

[1]L. D. Landau and J. B. Sykes, *Electrodynamics of Continuous Media* (Pergamon Press, Oxford, 1960).
[2]G. Srinivasan, E. T. Rasmussen, A. A. Bush, K. E. Kamentsev, V. F. Meshcheryakov, and Y. K. Fetisov, Appl. Phys. A **78**, 721 (2004).
[3]W. Eerenstein, N. D. Mathur, and J. F. Scott, Nature (London) **442**,759 (2006).
[4]S. X. Dong, J. F. Li, and D. Viehland, Appl. Phys. Lett. **85**, 5305 (2004).
[5]D. T. H. Giang, L. K. Quynh, N. Van Dung, and N. H. Nghi, in *Magnetoelectric Effects in Piezoelectric/Soft Magnetic Amorphous Feco-based Ribbon Composites* (IOP Publishing, 2009).
[6]C. W. Nan, M. I. Bichurin, S. X. Dong, D. Viehland, and G. Srinivasan, J. Appl. Phys. **103**, 031101 (2008).
[7]Z. P. Xing, S. X. Dong, J. Y. Zhai, L. Yan, J. F. Li, and D. Viehland, Appl. Phys. Lett. **89**, 112911 (2006).
[8]P. Li, Y. Wen, and L. Bian, Appl. Phys. Lett. **90**, 022503 (2007).
[9]J. H. Ryu, A. V. Carazo, K. J. Uchino, and H. E. Kim, Jpn. J. Appl. Phys., Part 1 **40**, 4948 (2001).
[10]D. A. Pan, Y. Bai, W. Y. Chu, and L. J. Qiao, Smart Mater. Struct. **16**, 2501 (2007).
[11]D. A. Pan, Y. Bai, A. A. Volinsky, W. Y. Chu, and L. J. Qiao, Appl. Phys. Lett. **92**, 052904 (2008).
[12]W. Wu, K. Bi, and Y. G. Wang, J. Mater. Sci. **46**, 1602 (2011).
[13]Z. J. Zuo, D. A. Pan, Y. M. Jia, S. G. Zhang, and L. J. Qiao, AIP Adv. **3**, 122114 (2013).
[14]S. X. Dong, J. Y. Zhai, J. F. Li, and D. Viehland, Appl. Phys. Lett. **89**, 122903 (2006).
[15]J. Y. Zhai, S. X. Dong, Z. P. Xing, J. F. Li, and D. Viehland, Appl. Phys. Lett. **89**, 083507 (2006).
[16]Z. Fang, S. G. Lu, F. Li, S. Datta, Q. M. Zhang, and M. El Tahchi, Appl. Phys. Lett. **95**, 112903 (2009).
[17]D. A. Pan, J. Wang, Z. J. Zuo, S. G. Zhang, L. J. Qiao, and A. A. Volinsky, Appl. Phys. Lett. **104**, 122903 (2014).
[18]J. Petzold, Scr. Mater. **48**, 895 (2003).
[19]W. Wu, Y. G. Wang, and K. Bi, J. Magn. Magn. Mater. **323**, 422 (2011).
[20]D. A. Pan, Y. Bai, W. Y. Chu, and L. J. Qiao, J. Phys. D: Appl. Phys. **41**, 022002 (2008).
[21]L. Chen, P. Li, Y. M. Wen, and D. Wang, Acta Phys. Sin. **60**, 067501 (2011) (in Chinese).
[22]S. X. Dong, J. Y. Zhai, J. F. Li, and D. Viehland, Appl. Phys. Lett. **89**, 252904 (2006).